8.30 (dd, 1.4, 8.1 Hz, J_{PtH} = 10.0 Hz); $^{13}C\{^1H\}$, δ(C) 0.01 ($SiMe_3$), 93.59 (J_{PtC} = 36.1 Hz, Cp), 94.20 (J_{PtC} = 20.2 Hz, Cp), 106.71 (ipso, Cp), 122.74, 124.48 (int 2), 124.87 (J_{PtC} = 58.0 Hz), 128.42 (int 2), 128.76 (int 2), 137.55 (J_{PtC} = 104.9 Hz), 156.87 (J_{PtC} = 105.8 Hz), 161.08 (J_{PtC} = 95.3 Hz), 165.74 (J_{PtC} = 1351.5 Hz).

Acknowledgment. We thank the donors of the Petroleum Research Fund, administered by the American Chemical Society, for financial support (G.K.A.), NATO for a travel grant (G.K.A. and R.J.C.), the NSF for an instrumentation grant (Grant No. CHE-8506671), and Johnson Matthey for a loan of palladium and platinum salts.

Synthesis and Structural Characterization of $(C_5Me_5)Zr(R)_2(L)_n^+$ Complexes

Donna J. Crowther, Richard F. Jordan,* Norman C. Baenziger, and Akhilkumar Verma

Department of Chemistry, University of Iowa, Iowa City, Iowa 52242

Received March 12, 1990

The reaction of $(C_5Me_5)Zr(CH_3)_3$ with $[(C_5H_4Me)_2Fe][BPh_4]$ in THF yields $[(C_5Me_5)Zr(CH_3)_2(THF)_2][BPh_4]$ (1) via oxidative cleavage of a Zr–CH_3 bond. X-ray diffraction reveals that the cation of **1** adopts a square-pyramidal/four-legged piano-stool structure with cis CH_3 groups. The orientations of the THF ligands and the Zr–O bond distances suggest that Zr–O π-bonding is important for at least one of the THF ligands. Data for **1**: a = 14.551 (2) Å, b = 15.191 (4) Å, c = 17.852 (19) Å, β = 92.26 (3)°, V = 3943 (6) Å^3, Z = 4 in space group $P2_1/c$. Reaction of **1** with excess dmpe in THF solution yields $[(C_5Me_5)Zr(CH_3)_2(dmpe)(THF)][BPh_4]$ (**2**), which also has been characterized by X-ray diffraction. The cation of **2** has a distorted-octahedral structure with the Cp* ligand in an axial position and equatorial/axial coordination of the dmpe ligand. The two CH_3 groups are equatorial and mutually trans. The THF ligand is equatorial and trans to the dmpe ligand and lies in the square plane in an orientation that precludes Zr–O π-bonding. Data for **2**: a = 10.110 (3) Å, b = 14.701 (8) Å, c = 17.190 (4) Å, α = 70.14 (3)°, β = 78.72 (2)°, γ = 84.68 (4)°, V = 2355.6 (1.9) Å^3, Z = 2 in space group $P\bar{1}$. The reaction of $(C_5Me_5)Zr(CH_2Ph)_3$ with $[(C_5H_4Me)_2Fe][BPh_4]$ in THF at 0 °C yields the thermally sensitive compound $[(C_5Me_5)Zr(CH_2Ph)_2(THF)][BPh_4]$ (**3**). The benzyl ligands of **3** are distorted, most likely as a result of weak donor interactions between the Ph rings and the cationic Zr center.

Cationic Zr(IV) alkyl complexes of general type $Cp^*_2Zr(R)^+$ (Cp^* = C_5Me_5) and $Cp_2Zr(R)(L)_n^+$ contain highly unsaturated Lewis-acidic metal centers, vacant coordination sites and/or labile ligands L, and reactive Zr–R bonds. This combination promotes insertion and σ-bond metathesis chemistry.[1-3] It is currently believed that cationic species of this type play a key role in metallocene-based olefin polymerization catalyst systems.[1-4] Cationic mono-C_5R_5 Zr(IV) alkyl complexes $(C_5R_5)Zr(R)_2(L)_n^+$ are of interest because their increased unsaturation may lead to even higher reactivity, particularly with sterically crowded substrates.[5,6] It is also possible that $(C_5R_5)M(R)_2^+$ species play a role in some $(C_5R_5)MX_3$-based olefin polymerization catalysts.[7] This paper describes the synthesis and characterization of several $(C_5Me_5)Zr(R)_2(L)_n^+$ complexes which are the first examples of this class.

Results and Discussion

Synthesis of $[Cp^*Zr(CH_3)_2(THF)_2][BPh_4]$ (1). The reaction of $Cp^*Zr(CH_3)_3$ with $[Cp'_2Fe][BPh_4]$ (Cp′ =

(1) (a) Jordan, R. F.; Dasher, W. E.; Echols, S. F. *J. Am. Chem. Soc.* **1986**, *108*, 1718. (b) Jordan, R. F.; Bajgur, C. S.; Willett, R.; Scott, B. *J. Am. Chem. Soc.* **1986**, *108*, 7410. (c) Jordan, R. F.; Echols, S. F. *Inorg. Chem.* **1987**, *26*, 383. (d) Jordan, R. F.; LaPointe, R. E.; Bajgur, C. S.; Echols, S. F.; Willett, R. *J. Am. Chem. Soc.* **1987**, *109*, 4111. (e) Jordan, R. F.; Bajgur, C. S.; Dasher, W. E.; Rheingold, A. L. *Organometallics* **1987**, *6*, 1041. (f) Jordan, R. F. *J. Chem. Educ.* **1988**, *65*, 285. (g) Jordan, R. F.; LaPointe, R. E.; Bradley P. K.; Baenziger, N. C. *Organometallics* **1989**, *8*, 2892. (h) Jordan, R. F.; LaPointe, R. E.; Baenziger, N. C.; Hinch, G. D. *Organometallics* **1990**, *9*, 1539. (i) Jordan, R. F.; Bradley, P. K.; Baenziger, N. C.; LaPointe, R. E. *J. Am. Chem. Soc.* **1990**, *112*, 1289. (j) Jordan, R. F.; Taylor, D. F. *J. Am. Chem. Soc.* **1989**, *111*, 778. (k) Jordan, R. F.; Taylor, D. F.; Baenziger, N. C. *Organometallics* **1990**, *9*, 1546. (l) Jordan, R. F.; Guram, A. S. *Organometallics* **1990**, *9*, 2116.

(2) Hlatky, G. G.; Turner, H. W.; Eckman, R. R. *J. Am. Chem. Soc.* **1989**, *111*, 2728.

(3) (a) Bochmann, M.; Wilson, L. M. *J. Chem. Soc., Chem. Commun.* **1986**, 1610. (b) Bochmann, M.; Wilson, L. M.; Hursthouse, M. B.; Short, R. L. *Organometallics* **1987**, *6*, 2556. (c) Bochmann, M.; Wilson, L. M.; Hursthouse, M. B.; Motevalli, M. *Organometallics* **1988**, *7*, 1148. (d) Bockmann, M.; Jaggar, A. J.; Wilson, L. M.; Hursthouse, M. B.; Motevalli, M. *Polyhedron* **1989**, *8*, 1838. (e) Taube, R.; Krukowka, L. *J. Organomet. Chem.* **1988**, *347*, C9.

(4) (a) Eisch, J. J.; Piotrowski, A. M.; Brownstein, S. K.; Gabe, E. J.; Lee, F. L. *J. Am. Chem. Soc.* **1985**, *107*, 7219. (b) Gassman, P. G.; Callstrom, M. R. *J. Am. Chem. Soc.* **1987**, *109*, 7875. (c) Hedden, D.; Marks, T. J. *J. Am. Chem. Soc.* **1988**, *110*, 1647. (d) Toscano, P. J.; Marks, T. J. *J. Am. Chem. Soc.* **1985**, *107*, 653. (e) Dyachkovskii, F. S.; Shilova, A. K.; Shilov, A. E. *J. Polym. Sci., Part C* **1967**, *16*, 2333. (f) Ewen, J. A.; Jones, R. L.; Razavi, A.; Ferrara, J. D. *J. Am. Chem. Soc.* **1988**, *110*, 6255. (g) Pino, P.; Cioni, P.; Wei, J. *J. Am. Chem. Soc.* **1987**, *109*, 6189.

(5) For leading references to neutral mono-C_5R_5 group 4 metal alkyl complexes and related complexes see: (a) Wolczanski, P. T.; Bercaw, J. E. *Organometallics* **1982**, *1*, 793. (b) Wengrovius, J. R.; Schrock, R. R. *J. Organomet. Chem.* **1981**, *205*, 319. (c) Blenkers, J.; DeLiefde Meijer, H. J.; Teuben, J. H. *J. Organomet. Chem.* **1981**, *218*, 383. (d) Mintz, E. A.; Moloy, K. G.; Marks, T. J.; Day, V. W. *J. Am. Chem. Soc.* **1982**, *104*, 4692. (e) Erker, G.; Berg, K.; Angermund, K.; Kruger, C. *Organometallics* **1987**, *6*, 2620. (f) Mena, M.; Royo, P.; Serrano, R.; Pellinghelli, M. A.; Tiripicchio, A. *Organometallics* **1989**, *8*, 476. (g) Mena, M.; Pellinghelli, M. A.; Royo, P.; Serrano, R.; Tiripicchio, A. *J. Chem. Soc., Chem. Commun.* **1986**, 1118. (h) Roddick, D. M.; Santarsiero, B. D.; Bercaw, J. E. *J. Am. Chem. Soc.* **1985**, *107*, 4670. (i) Wielstra, Y.; Gambarotta, S.; Roedelof, J. B.; Chiang, M. C. *Organometallics* **1988**, *7*, 2177.

(6) For related lanthanide alkyls of the type $(C_5R_5)M(R)_2(L)_n$, see: (a) van der Heijden, H.; Pasman, P.; de Boer, E. J. M.; Schaverien, C. J. *Organometallics* **1989**, *8*, 1459. (b) van der Heijden, H.; Schaverien, C. J.; Orpen, A. G. *Organometallics* **1989**, *8*, 255. (c) Heeres, H. J.; Meetsma, A.; Teuben, J. H.; Rogers, R. D. *Organometallics* **1989**, *8*, 2637. (d) See also: Schumann, H.; Albrecht, I.; Pickardt, J.; Hahn, E. *J. Organomet. Chem.* **1984**, *276*, C5. (e) Albrecht, I.; Schumann, H. *J. Organomet. Chem.* **1986**, *310*, C29.

(7) (a) Dahmen, K.-H.; Hedden, D.; Burwell, R. L.; Marks, T. J. *Langmuir* **1988**, *4*, 1212. (b) Ishihara, N.; Kuramoto, M.; Uoi, M. *Macromolecules* **1988**, *21*, 3356. (c) Zambelli, A.; Oliva, L.; Pellecchia, C. *Macromolecules* **1989**, *22*, 2129. (d) Chien, J. C. W.; Wang, B.-P. *J. Polym. Sci., Part A* **1989**, *27*, 1539. (e) Skupinski, W.; Cieslowska-Glinska, I.; Wasilewski, A. *J. Mol. Catal.* **1985**, *33*, 129.

0276-7333/90/2309-2574$02.50/0

Table I. Selected Bond Distances (Å) and Angles (deg) for $[Cp^*ZrMe_2(THF)_2][BPh_4]$ (1)

Bond Distances			
Zr–C1C[a]	2.200	C23–C22	1.51 (2)
Zr–C31	2.270 (9)	C22–O21	1.46 (1)
Zr–C32	2.22 (1)	C1–C2	1.43 (1)
Zr–O11	2.243 (5)	C2–C3	1.40 (1)
Zr–O21	2.302 (5)	C3–C4	1.42 (1)
O11–C15	1.48 (1)	C4–C5	1.40 (1)
C15–C14	1.48 (1)	C5–C1	1.38 (1)
C14–C13	1.49 (1)	C1–C6	1.52 (1)
C13–C12	1.53 (1)	C2–C7	1.52 (1)
C12–O11	1.46 (1)	C3–C8	1.49 (1)
O21–C25	1.48 (1)	C4–C9	1.51 (1)
C25–C24	1.39 (2)	C5–C10	1.48 (1)
C24–C23	1.40 (2)		
Bond Angles			
C1C–Zr–C32	108.3	O21–Zr–O11	73.9 (2)
C1C–Zr–C31	108.6	Zr–O21–C25	128.2 (6)
C1C–Zr–O21	115.4	Zr–O21–C22	124.0 (6)
C1C–Zr–O11	120.4	Zr–O11–C12	127.3 (5)
C32–Zr–C31	87.4 (4)	Zr–O11–C15	116.6 (5)
C32–Zr–O21	82.5 (3)	C22–O21–C25	107.7 (7)
C31–Zr–O11	81.3 (3)	C15–O11–C12	108.4 (6)
C31–Zr–O21	135.8 (3)	C32–Zr–O11	131.2 (3)

[a] ClC denotes the Cp* ring centroid.

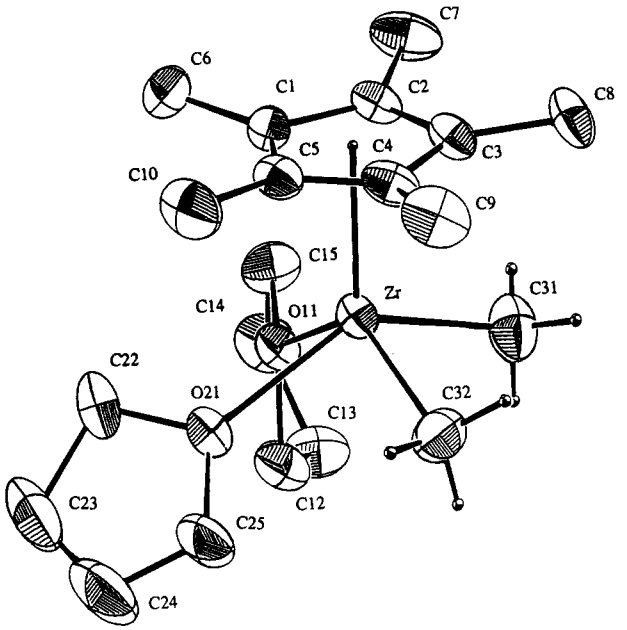

Figure 1. Ortep view of the cation of 1.

C_5H_4Me) in THF produces $[Cp^*Zr(CH_3)_2(THF)_2][BPh_4]$ (1), which is isolated by precipitation with Et_2O followed by recrystallization from THF/Et_2O (55%, eq 1). Bis-

$$Cp^*Zr(CH_3)_3 + [Cp'_2Fe][BPh_4] \xrightarrow[-Cp'_2Fe]{THF} \underset{1}{[Cp^*Zr(CH_3)_2(THF)_2][BPh_4]} \quad (1)$$

(methylcyclopentadienyl)iron(II) (Cp_2Fe) is also produced in this reaction; the organic byproducts were not determined. The ^1H and ^{13}C NMR spectra of 1 in THF-d_8 solution are temperature-independent and establish that the Zr–CH_3 groups are equivalent. The ^1H NMR spectra contain resonances for free THF (2 equiv), which establishes that isolated 1 contains 2 equiv of THF. Low-temperature ^1H and ^{13}C NMR spectra do not exhibit resonances for coordinated THF or THF-d_8, indicating that ligand exchange is rapid on the NMR time scale. As a result, the nature and number of THF ligands in 1 in THF solution is unknown. However, the structure of 2 (vide infra) suggests that 1 may coordinate a third THF in solution. Complex 1 is stable in THF solution at ambient temperature, is insoluble in Et_2O and hydrocarbon solvents, and decomposes in CH_2Cl_2 solution, presumably by chloride abstraction from the solvent.

Table II. Positional Parameters for $[Cp^*ZrMe_2(THF)_2][BPh_4]$ (1)

atom	x	y	z	B,[a] Å²
Zr	−0.18042 (5)	0.18441 (5)	−0.09429 (4)	4.11 (2)
O11	−0.2996 (3)	0.1657 (3)	−0.1763 (3)	4.7 (1)
O21	−0.2389 (4)	0.0468 (4)	−0.0707 (3)	5.7 (1)
C1	−0.2707 (6)	0.2687 (6)	−0.0039 (5)	5.0 (2)
C2	−0.2215 (6)	0.3335 (5)	−0.0445 (5)	4.5 (2)
C3	−0.1280 (6)	0.3229 (5)	−0.0266 (5)	4.8 (2)
C4	−0.1193 (6)	0.2531 (5)	0.0258 (5)	5.1 (2)
C5	−0.2072 (6)	0.2207 (6)	0.0386 (5)	5.1 (2)
C6	−0.3745 (7)	0.2658 (8)	0.0004 (6)	7.5 (3)
C7	−0.2632 (8)	0.4073 (6)	−0.0918 (6)	7.4 (3)
C8	−0.0527 (7)	0.3802 (7)	−0.0530 (6)	6.9 (2)
C9	−0.0316 (8)	0.2263 (8)	0.0677 (6)	7.8 (3)
C10	−0.2257 (9)	0.1525 (8)	0.0956 (6)	8.8 (3)
C12	−0.3634 (6)	0.2329 (7)	−0.2052 (6)	6.4 (2)
C13	−0.3952 (7)	0.2010 (7)	−0.2830 (6)	7.3 (3)
C14	−0.3189 (7)	0.1427 (7)	−0.3059 (5)	6.9 (2)
C15	−0.2881 (7)	0.0986 (6)	−0.2357 (6)	6.2 (2)
C22	−0.3352 (7)	0.0295 (7)	−0.0561 (7)	8.3 (3)
C23	−0.3428 (9)	−0.0693 (8)	−0.0594 (8)	10.6 (4)
C24	−0.255 (1)	−0.1039 (8)	−0.067 (1)	12.8 (5)
C25	−0.1889 (8)	−0.0378 (7)	−0.0647 (8)	8.8 (3)
C31	−0.1218 (7)	0.2534 (8)	−0.1946 (5)	7.5 (3)
C32	−0.0474 (7)	0.1139 (7)	−0.0809 (6)	7.0 (3)
C41	0.3767 (5)	0.1106 (5)	0.3648 (4)	3.9 (2)*
C42	0.4241 (5)	0.0478 (5)	0.4091 (4)	4.4 (2)*
C43	0.5013 (6)	0.0014 (6)	0.3830 (5)	5.9 (2)*
C44	0.5300 (6)	0.0169 (6)	0.3133 (5)	5.6 (2)*
C45	0.4849 (6)	0.0747 (6)	0.2665 (5)	5.5 (2)*
C46	0.4074 (6)	0.1215 (6)	0.2929 (5)	4.9 (2)*
C51	0.2819 (5)	0.1631 (5)	0.4850 (4)	3.3 (1)*
C52	0.3578 (5)	0.1872 (5)	0.5277 (5)	4.5 (2)*
C53	0.3583 (6)	0.1950 (6)	0.6078 (5)	5.7 (2)*
C54	0.2825 (6)	0.1755 (6)	0.6431 (5)	5.8 (2)*
C55	0.2043 (6)	0.1514 (6)	0.6058 (5)	5.5 (2)*
C56	0.2048 (5)	0.1447 (6)	0.5256 (5)	4.7 (2)*
C61	0.1974 (5)	0.1047 (5)	0.3543 (4)	4.0 (2)*
C62	0.1737 (5)	0.0220 (6)	0.3829 (5)	4.9 (2)*
C63	0.1041 (6)	−0.0298 (7)	0.3492 (5)	6.2 (2)*
C64	0.0573 (7)	−0.0012 (7)	0.2882 (6)	6.5 (2)*
C65	0.0783 (6)	0.0754 (6)	0.2582 (5)	6.1 (2)*
C66	0.1501 (6)	0.1283 (6)	0.2889 (5)	5.1 (2)*
C71	0.2863 (5)	0.2640 (5)	0.3683 (4)	4.3 (2)*
C72	0.2062 (6)	0.3144 (6)	0.3584 (5)	5.2 (2)*
C73	0.2073 (7)	0.4042 (7)	0.3401 (6)	6.6 (2)*
C74	0.2888 (7)	0.4440 (7)	0.3318 (6)	7.0 (2)*
C75	0.3694 (7)	0.3986 (7)	0.3429 (6)	6.4 (2)*
C76	0.3677 (6)	0.3092 (6)	0.3608 (5)	5.2 (2)*
B	0.2843 (6)	0.1607 (6)	0.3924 (5)	3.4 (2)*
C1C	−0.1892	0.2799	−0.0022	0*

[a] Starred values denote atoms refined isotropically. Anisotropically refined atoms are given in the form of the isotropic equivalent displacement parameter defined as $^4/_3[a^2B_{11} + b^2B_{22} + c^2B_{33} + ab(\cos\gamma)B_{12} + ac(\cos\beta)B_{13} + bc(\cos\alpha)B_{23}]$.

Structure of 1. A single-crystal X-ray diffraction analysis of 1 was performed to elucidate the details of the cation structure. Metrical parameters and atomic coordinates are listed in Tables I and II. The $Cp^*Zr(CH_3)_2(THF)_2^+$ cation adopts a square-pyramidal/four-legged piano-stool structure (Figure 1) with the Cp* ligand in the apical site and a cis arrangement of CH_3 and THF ligands. The Zr atom is 0.88 Å out of the plane defined by the donor atoms of the THF and CH_3 ligands, and the Zr–Cp* and Zr–C distances are in the range observed for related mono- and bis-Cp complexes.[1,5] The angle between the Cp* plane and the C31–C32–O21–O11 square plane is 5.8°.

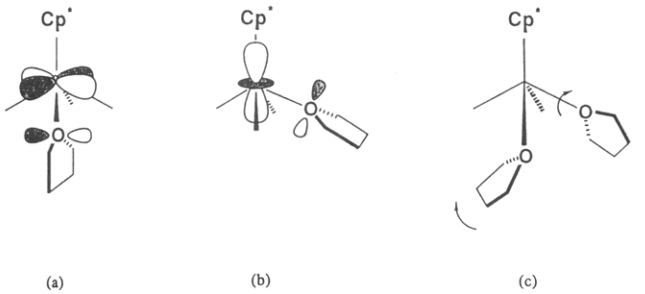

Figure 2. (a) Idealized geometry for maximum π-bonding between THF and Zr d_{xy} orbital. (b) Idealized geometry for maximum π-bonding between THF and Zr d_{z^2} orbital. (c) Actual orientation of THF ligands in **1** due to steric interactions.

The C32 methyl group eclipses the C9 Cp* CH_3 group, while the C31 CH_3 and THF ligands lie between Cp* CH_3 groups.

The orientation of the THF ligands of **1** is interesting and provides insight to the interplay of electronic and steric effects in this complex. One THF ligand (O21) is essentially flat at O and is oriented so that the dihedral angle between the C22–O21–C25 plane and the C31–C32–O21–O11 square plane is 37.2°. The second THF (O11) is distorted from a flat geometry at O (the angle between the O11–Zr bond and the C12–O11–C15 plane is 25°) and is essentially perpendicular to the square plane (dihedral angle between the C12–O11–C15 plane and the square plane is 85.0°). A d^0 $CpML_4$ complex contains two low-lying metal LUMO's which are mostly d_{xy} and d_{z^2} in character.[8] An idealized structure (Figure 2) in which the THF C–O–C planes are rotated 90° (Figure 2a) and 0° (Figure 2b), relative to the square plane, allows maximum π-donation to these orbitals. The observed structure of **1** is derived from this ideal structure by rotation about Zr–O21 bond (leading to the 37.2° dihedral angle) and by twisting about O11 (leading to some pyramidalization) as illustrated in Figure 2c. The source of these distortions is probably steric crowding between the two cis THF ligands. The rotation about the Zr–O21 bond also allows some π-donation from O21 to the Zr d_{xy} orbital. The Zr–O11 distance (2.243 (5) Å) is significantly shorter than the Zr–O21 distance (2.302 (5) Å), suggesting that π-donation is stronger from O11 despite the pyramidalization. This is consistent with overlap considerations which suggest that π-bonding involving the Zr d_{xy} orbital (and O11) should be stronger than π-bonding involving the d_{z^2} orbital (and O21). However, this difference may also reflect in part a difference in Zr–O σ-bond strength. The Zr–THF distances in related cationic $Cp_2Zr(R)(THF)^+$ complexes are quite variable and appear to be related to the extent of Zr–O π-bonding. For example, the Zr–O distance is quite short (2.122 (14) Å) in $Cp_2Zr(CH_3)(THF)^+$, in which the THF is in a near-optimum orientation for π-bonding.[1b] The THF ligand in $(C_5H_4Me)_2Zr\{(Z)\text{-}C(Me)=C(^iPr)(Me)\}(THF)^+$ is rotated 45° from the optimum orientation for π-bonding, and the Zr–O distance is correspondingly long (2.289 (6) Å).[1g] The Zr–O distances in **1** are significantly shorter than the Zr–O distances of 2.31–2.39 Å in *mer*-$(C_5H_4R)ZrCl_3(THF)_2$ (R = H, Me) complexes, which contain π-donor Cl^- ligands and are neutral.[9]

There is no evidence for agostic or distorted CH_3 groups in **1**. The observed J_{CH} value of 117 Hz is typical of d^0 metal alkyl complexes and nearly identical with the J_{CH} = 116 Hz observed for the α-carbons of $(C_5H_4Me)_2Zr(R)(THF)^+$ (R = CH_3, Et, ^{n}Bu), which contain undistorted alkyl ligands.[1g] A larger value for J_{CH} might be expected for an agostic structure on the basis of the observed J_{CH} = 129.5 Hz for $Ti(dmpe)Cl_3Me$.[10] Also, no low-energy ν_{CH} bands are observed in the IR spectrum of **1**. The positions of the methyl hydrogens, as estimated from electron density difference maps (see Experimental Section), indicate that the Me groups are not grossly distorted. Presumably the π-donation from the THF ligands precludes Zr–H–C interactions.

Table III. Selected Bond Distances (Å) and Angles (deg) for $[Cp^*ZrMe_2(dmpe)(THF)][BPh_4]$ (2)

Bond Distances			
Zr–C1C[a]	2.258	P1–C21	1.82 (1)
Zr–C31	2.32 (1)	P2–C26	1.86 (2)
Zr–C32	2.31 (1)	P2–C22	1.79 (2)
Zr–O11	2.280 (6)	P2–C24	1.83 (2)
Zr–P1	2.811 (3)	C1–C2	1.40 (2)
Zr–P2	2.850 (3)	C2–C3	1.42 (2)
C15–C14	1.53 (2)	C3–C4	1.42 (2)
C14–C13	1.48 (2)	C4–C5	1.41 (2)
C13–C12	1.49 (2)	C5–C1	1.42 (1)
C12–O11	1.47 (1)	C1–C6	1.52 (2)
O11–C15	1.45 (1)	C2–C7	1.51 (2)
P1–C25	1.78 (2)	C3–C8	1.51 (2)
P1–C23	1.83 (2)	C4–C9	1.51 (2)
		C5–C10	1.49 (2)
Bond Angles			
C1C–Zr–C32	105.5	O11–Zr–C32	93.9 (3)
C1C–Zr–C31	105.2	P2–Zr–P1	72.2 (1)
C1C–Zr–O11	103.9	P2–Zr–O11	75.5 (2)
C1C–Zr–P1	108.4	P2–Zr–C31	74.6 (3)
C1C–Zr–P2	179.2	P2–Zr–C32	75.0 (3)
C31–Zr–C32	143.2 (4)	Zr–P1–C25	108.7 (5)
P1–Zr–C31	76.0 (3)	Zr–P2–C26	107.7 (5)
P1–Zr–C32	75.4 (3)	C12–O11–C15	108.6 (8)
P1–Zr–O11	147.6 (2)	C13–C12–O11	106.2 (1.0)
O11–Zr–C31	98.0 (3)	O11–C15–C14	106.0 (9)

[a] C1C denotes the Cp* ring centroid.

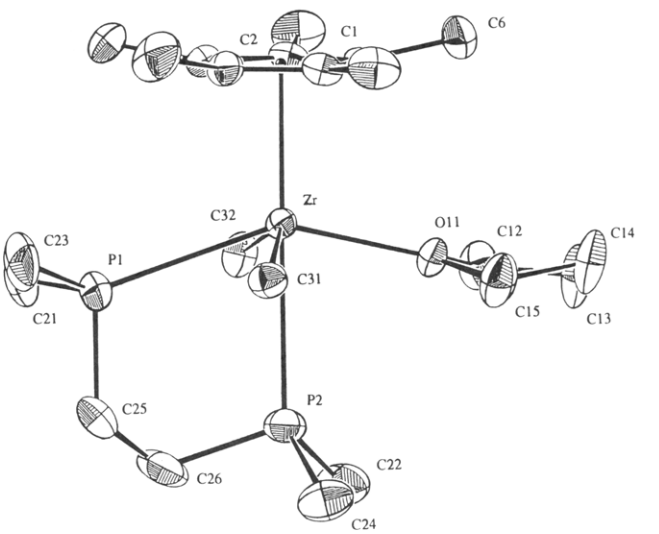

Figure 3. Ortep view of the cation of **2**.

Synthesis and Structure of $[Cp^*Zr(CH_3)_2(dmpe)(THF)][BPh_4]$ (2). The reaction of **1** with $Me_2PCH_2CH_2PMe_2$ (dmpe) in THF solution produces

(8) (a) Kubacek, P.; Hoffmann, R.; Havlas, Z. *Organometallics* **1982**, *1*, 180. (b) Green, J. C. *Struct. Bonding (Berlin)* **1981**, *43*, 37.

(9) Erker, G.; Sarter, C.; Albrecht, M.; Dehnicke, S.; Kruger, C.; Raabe, E.; Schlund, R.; Benn, R.; Rufinska, A.; Mynott, R. *J. Organomet. Chem.* **1990**, *382*, 79.

(10) Dawoodi, Z.; Green, M. L. H.; Mtetwa, V. S. B.; Prout, K.; Schultz, A. J.; Williams, J. M.; Koetzle, T. F. *J. Chem. Soc., Dalton, Trans.* **1986**, 1629.

Table IV. Positional Parameters for [Cp*ZrMe$_2$(dmpe)(THF)][BPh$_4$] (2)

atom	x	y	z	B,[a] Å^2
Zr	0.2170 (1)	−0.19847 (7)	0.22006 (5)	2.91 (2)
P1	0.1891 (3)	−0.3047 (2)	0.1159 (2)	4.81 (8)
P2	−0.0597 (3)	−0.1857 (3)	0.2033 (2)	5.08 (8)
O11	0.1140 (7)	−0.1113 (5)	0.3035 (4)	4.0 (2)
O81S	0.254	0.255	0.494	5.8 (7)*
O91S	0.355	0.276	0.368	10 (1)*
C1	0.407 (1)	−0.1675 (8)	0.2855 (6)	3.9 (3)
C2	0.409 (1)	−0.2677 (8)	0.3014 (6)	4.1 (3)
C3	0.450 (1)	−0.2843 (8)	0.2235 (6)	4.5 (3)
C4	0.471 (1)	−0.1931 (8)	0.1596 (6)	4.2 (3)
C5	0.443 (1)	−0.1209 (8)	0.1978 (6)	4.0 (3)
C6	0.397 (1)	−0.1213 (9)	0.3530 (7)	6.6 (4)
C7	0.398 (1)	−0.345 (1)	0.3865 (8)	6.6 (4)
C8	0.490 (1)	−0.3808 (9)	0.2110 (9)	7.5 (4)
C9	0.540 (2)	−0.177 (1)	0.0700 (8)	7.8 (5)
C10	0.463 (1)	−0.0153 (9)	0.1547 (8)	6.4 (4)
C12	0.052 (1)	−0.1512 (9)	0.3923 (6)	5.7 (3)
C13	0.014 (2)	−0.067 (1)	0.4221 (8)	8.1 (5)
C14	0.069 (2)	0.0217 (9)	0.3549 (8)	7.8 (5)
C15	0.091 (2)	−0.0070 (9)	0.2758 (7)	6.5 (4)
C21	0.189 (2)	−0.4366 (9)	0.1578 (8)	7.4 (4)
C22	−0.193 (1)	−0.216 (1)	0.2931 (9)	7.7 (5)
C23	0.292 (2)	−0.283 (1)	0.0116 (7)	8.5 (5)
C24	−0.132 (2)	−0.074 (1)	0.138 (1)	8.2 (5)
C25	0.026 (1)	−0.278 (1)	0.0867 (7)	7.3 (4)
C26	−0.086 (1)	−0.278 (1)	0.1564 (8)	7.5 (4)
C31	0.205 (1)	−0.0809 (8)	0.0907 (6)	4.3 (3)
C32	0.128 (1)	−0.3433 (8)	0.3117 (7)	4.9 (3)
C41	0.781 (1)	0.2091 (7)	0.2979 (5)	3.3 (2)*
C42	0.736 (1)	0.1562 (8)	0.2571 (7)	4.9 (3)*
C43	0.668 (1)	0.0670 (9)	0.3014 (7)	6.0 (3)*
C44	0.642 (1)	0.0347 (9)	0.3858 (7)	5.9 (3)*
C45	0.685 (1)	0.0850 (9)	0.4289 (7)	5.3 (3)*
C46	0.755 (1)	0.1725 (7)	0.3849 (6)	4.0 (2)*
C51	0.871 (1)	0.3676 (7)	0.3117 (6)	3.5 (2)*
C52	0.955 (1)	0.3364 (8)	0.3724 (6)	4.1 (2)*
C53	0.954 (1)	0.3857 (8)	0.4311 (7)	5.3 (3)*
C54	0.871 (1)	0.4637 (9)	0.4297 (7)	5.3 (3)*
C55	0.792 (1)	0.4972 (9)	0.3715 (7)	5.4 (3)*
C56	0.794 (1)	0.4505 (8)	0.3116 (6)	4.2 (2)*
C61	0.789 (1)	0.3799 (7)	0.1697 (6)	3.4 (2)*
C62	0.651 (1)	0.3789 (8)	0.1703 (6)	4.1 (2)*
C63	0.587 (1)	0.4450 (8)	0.1089 (6)	4.7 (3)*
C64	0.660 (1)	0.5180 (8)	0.0469 (6)	4.5 (2)*
C65	0.796 (1)	0.5224 (8)	0.0449 (6)	4.4 (2)*
C66	0.858 (1)	0.4550 (7)	0.1053 (6)	4.0 (2)*
C71	1.015 (1)	0.2804 (7)	0.2020 (5)	3.3 (2)*
C72	1.028 (1)	0.2330 (8)	0.1444 (7)	4.8 (3)*
C73	1.156 (1)	0.2069 (9)	0.1035 (7)	5.3 (3)*
C74	1.271 (1)	0.2303 (9)	0.1201 (7)	5.6 (3)*
C75	1.266 (1)	0.2790 (9)	0.1748 (8)	6.1 (3)*
C76	1.135 (1)	0.3031 (8)	0.2155 (7)	4.9 (3)*
C82S	0.376	0.287	0.504	4 (1)*
C83S	0.391	0.291	0.361	6 (1)*
C84S	0.449	0.337	0.415	8 (2)*
C85S	0.290	0.219	0.425	6 (1)*
C92S	0.324	0.206	0.450	7 (1)*
C93S	0.279	0.266	0.509	9 (2)*
C94S	0.345	0.364	0.461	5 (1)*
C95S	0.422	0.350	0.380	6 (1)*
B	0.868 (1)	0.3083 (8)	0.2465 (7)	3.2 (2)*

[a] See footnote *a* of Table II.

[Cp*Zr(Me)$_2$(THF)(dmpe)][BPh$_4$] (**2**), which is isolated by precipitation with Et_2O followed by recrystallization from THF/Et_2O (82%, eq 2). The solid-state structure

$$\underset{\mathbf{1}}{Cp^*Zr(CH_3)_2(THF_2)^+} + PMe_2CH_2CH_2PMe_2 \rightarrow \underset{\mathbf{2}}{Cp^*Zr(CH_3)_2(dmpe)(THF)^+} \quad (2)$$

of **2** was determined by X-ray diffraction. Metrical parameters and atomic coordinates are listed in Tables III and IV. The cation of **2** adopts the distorted-octahedral structure shown in Figure 3. The Cp* ligand occupies an axial site, and the dmpe ligand is coordinated in an axial/equatorial fashion, as observed for several related mono-Cp* and mono-Cp group 4 metal complexes.[11] The equatorial CH_3 groups are mutually trans and are bent away slightly from the THF ligand (the O–Zr–CH_3 angles are 98.0 (3) and 93.9 (3)°). The Zr–Cp* centroid distance (2.258 Å) and Zr–CH_3 distances (2.32 (1), 2.31 (1) Å) are ca. 0.06 Å longer than the corresponding distances in the 5-coordinate complex **1**, consistent with the decreased metal Lewis acidity and increased crowding expected in a 6-coordinate complex. The THF ligand eclipses the C6 Cp* CH_3 group, while the Zr–CH_3 and Zr–P1 ligands lie between Cp* CH_3 groups. The Zr atom is 0.64 (1) Å out of the P1–C31–O11–C32 square plane, and the dihedral angle between the square plane and the Cp* plane is 4.4 (7)°. The Zr–P2(axial) distance is 0.04 Å longer than the Zr–P1(equatorial) distance, consistent with the expected stronger trans effect of Cp* vs the THF ligand. For comparison, the Zr–O distance for the THF trans to Cp in $CpZrCl_3(THF)_2$ is 0.079 Å longer than the Zr–O distance for the cis THF.[9]

The THF ligand is coordinated in an equatorial position, contains an essentially flat O, and lies in the square plane (the dihedral angle between the C13–C12–O11–C15 plane and the P1–C31–O11–C32 square plane is 8.6 (7)°). This orientation precludes Zr–O π-bonding, as the THF b_2 π-donor orbital is orthogonal to the Zr LUMO (d_{xy}). Evidently the perpendicular orientation of the THF ligand in which π-bonding would be maximized is disfavored by steric crowding involving the Cp* and dmpe ligands. The Zr–O distance of 2.280 (6) Å is intermediate between the Zr–O bond distances in **1**; however detailed comparison is difficult due to the different structures and compositions of these complexes.

There is no evidence for Zr–H–C agostic interactions involving the Zr–CH_3 group of **2**. The J_{CH} value is normal (115 Hz), and there are no low-energy ν_{CH} bands in the IR spectrum. The X-ray data do not allow meaningful conclusions to be made about the positions of the Zr–CH_3 hydrogens.

Solution Behavior of 2. NMR spectroscopy establishes that at low temperature in THF solution (i) complex **2** maintains the solid-state structure and (ii) exchange of free and coordinated THF is slow on the NMR time scale. The ^{1}H spectrum (THF-d_8, −56 °C) contains a triplet for the ZrCH_3 groups and two PCH_3 doublets; the dmpe methylene resonances are obscured. Resonances for free THF are observed, indicating that exchange of THF with THF-d_8 solvent is rapid on the laboratory time scale (room-temperature sample preparation). The $^{13}C\{^1H\}$ spectrum (THF-d_8, −45 °C) contains a single ZrCH_3 resonance, two PCH_3 resonances, and two PCH_2 resonances. This spectrum establishes that the ZrCH_3 groups are equivalent, the sides of the dmpe ligand are equivalent, and the ends of the dmpe ligand are inequivalent, consistent with the solid-state structure. The presence of coordinated THF-d_8 is established by a ^{13}C resonance at δ 73.6 assigned to the α-CD_2; the β-CD_2 resonance is insufficiently shifted from that of free THF-d_8 or is too broad to be observed. The ^{31}P spectrum (−40 °C) consists of two doublets (δ −9.7, −10.0, J_{PP} = 11.4 Hz) shifted substantially downfield from the resonance for free dmpe (δ −47).

(11) (a) Stein, B. K.; Frerichs, S. R.; Ellis, J. E. *Organometallics* **1987**, *6*, 2017. (b) Wielstra, Y.; Gambarotta, S.; Meetsma, A.; L. de Boer, J.; Chiang, M. Y. *Organometallics* **1989**, *8*, 2696. (c) Hughes, D. L.; Leigh, G. J.; Walker, D. G. *J. Organomet. Chem.* **188**, *355*, 113.

Table V. Summary of Crystallographic Data for 1 and 2

compd	1	2
empirical formula	$C_{44}H_{57}BO_2Zr$	$C_{46}H_{65}BO_2P_2Zr\cdot0.5THF$
fw	719.97	834.0
cryst size, mm	0.26 × 0.30 × 0.41	0.20 × 0.30 × 0.40
cryst color	yellow	yellow
T, K	295	295
space group	$P2_1/c$	$P\bar{1}$
a, Å	14.551 (2)	10.110 (3)
b, Å	15.191 (4)	14.701 (8)
c, Å	17.852 (19)	17.190 (4)
α, deg		70.14 (3)
β, deg	92.26 (3)	78.72 (2)
γ, deg		84.68 (4)
V, Å^3	3943 (6)	2355.6 (1.9)
Z	4	2
d(calcd), g/cm^3	1.212	1.176
cell dimens	25 rflns, 12–28° (2θ)	20 rflns, 20–38° (2θ)
radiation	Mo Kα (λ = 0.71073 Å)	Mo Kα (λ = 0.71073 Å)
scan ratio, $2\theta/\omega$	0.7	1.33
scan limit, deg	$2 \le 2\theta \le 40$	$2 \le 2\theta \le 40$
scan speed, deg/min	1.2–5.0	0.75–4.0
scan range	0.8 + 0.35 tan θ	0.9 + 0.35 tan θ
data collected	$\pm h,-k,\pm l$	$\pm h,\pm k,\pm l$
no. of rflns collected	7718	7172
no. of unique rflns	3673	4388
decay (F^2), %	3.3	28
agrmnt btwn equiv rflns, %	2.2 (on F)	4.0 (on F)
no. of rflns with $I > 3\sigma(I)$	2627	2835
μ, cm^{-1}	2.98	3.28
abs cor (empirical on F)	max 1.00, min 0.97	max 1.00, min 0.67
structure soln	Patterson and DIRDIF	Patternson and DIRDIF
refinement	anisotropic on all non-H in cation; isotropic on anion; fixed H	anisotropic on all non-H in cation; isotropic on anion; fixed H
data/param in LS	2627/308	2835/345
R^a	0.054	0.068
$R_w{}^b$	0.088	0.096
weight (Killean and Lawrence)^c	P = 0.06, Q = 2.0	P = 0.07, Q = 1.0
SDOUW^d	1.17	1.14
max param shift/esd	0.09	0.19
max resid e density, e/Å^3	0.5	0.15

$^a R = \sum\Delta F_H/\sum F_{o,H}$, where $H = h, k, l$ and F_o is scaled to F_c. ΔF is $||F_o|-|F_c||$. $^b [R_w]^2 = \sum w(\Delta F_H)^2/\sum w(F_{o,H})^2$. ^{c} Killean and Lawrence weights are $1/(S^2 + (PF)^2 + Q)$, where S is the esd in F from counting statistics. If several octants are averaged, S is the larger of two estimates—one based on counting statistics, the other based on the agreement between equivalent reflections. esd = estimated standard deviation (Killean, R. C. G.; Lawrence, J. L. *Acta Crystallogr.* **1969**, *B25*, 1750). ^{d} SDOUW = standard deviation in an observation of unit weight.

Variable-temperature NMR spectroscopy reveals the presence of several exchange processes for **2**. The 23 °C $^{13}C\{^1H\}$ spectrum does not exhibit resonances for coordinated THF-d_8, indicating that exchange of coordinated and free THF-d_8 is rapid at this temperature. The 39 °C ^1H spectrum contains a broad singlet for the PCH_3 groups and a triplet for the $ZrCH_3$ groups, and the 40 °C $^{31}P\{^1H\}$ spectrum consists of a broad singlet. These results indicate that the two ends of the dmpe ligand undergo rapid site exchange at elevated temperature. The reversible THF exchange process in eq 3, which involves a square-pyramidal intermediate of C_s symmetry analogous to **1**, accommodates these observations. Interestingly, as the temperature is raised from −60 to +40 °C, the upfield ^{31}P

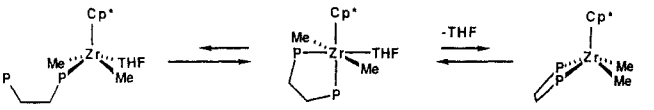

(3)

resonance broadens more than the downfield resonance, and the upfield ^1H PCH_3 resonance broadens more than its downfield partner, prior to coalescence. These observations suggest that in addition to the THF exchange process described above, **2** also undergoes reversible dissociation of one end of the dmpe ligand. On the basis of Erker's report that exchange of free and coordinated L in *mer*-$CpZrCl_3L_2$ complexes is faster for the L trans to Cp,[9] we propose that the axial end of the dmpe undergoes reversible exchange as indicated in eq 3. An exchange process (suggested by a reviewer) involving reversible THF dissociation and formation of *trans*-$Cp^*Zr(CH_3)_2(dmpe)^+$ (CH_3 groups mutually trans and trans coordination of dmpe) is also consistent with the NMR results.

Synthesis and Characterization of $[Cp^*Zr(CH_2Ph)_2(THF)][BPh_4]$ (3). The reaction of $Cp^*Zr(CH_2Ph)_3$ with $[Cp'_2Fe][BPh_4]$ at 0 °C yields $[Cp^*Zr(CH_2Ph)_2(THF)][BPh_4]$ (**3**, 86%) via oxidative cleavage of a benzyl ligand (eq 4). Higher reaction temperatures

$$Cp^*Zr(CH_2Ph)_3 + [Cp'_2Fe][BPh_4] \xrightarrow{THF,\ 0°C} \underset{\mathbf{3}}{[Cp^*Zr(CH_2Ph)_2(THF)][BPh_4]} + Cp'_2Fe + 0.5PhCH_2CH_2Ph \quad (4)$$

result in lower yields. Complex **3** is isolated as a yellow, thermally sensitive solid following evaporation of solvent, removal of Cp'_2Fe and bibenzyl via a toluene wash, and recrystallization from THF/Et_2O. At 23 °C, **3** decomposes (ca. 30% in 20 h) in THF solution to yield a mixture of BPh_3, $Cp^*Zr(CH_2Ph)_3$, and other organometallic products as well as some toluene and bibenzyl. The observation of the former products suggests that Ph^- abstraction from BPh_4^- by $Cp^*Zr(CH_2Ph)_2(THF)^+$ followed by disproportionation of the resulting $Cp^*Zr(Ph)(CH_2Ph)_2$ is a major decomposition mode. However, this decomposition process was not studied in detail due to its complexity. Complex **3** is also unstable in CH_2Cl_2 and is insoluble in hydrocarbons.

Unsaturated early-transition-metal benzyl complexes often exhibit distorted benzyl structures resulting from interactions of the Ph π-system (η^2- or η^n-benzyl) or a methylene C–H bond (agostic interaction) with a metal LUMO.[1d,g,h,5d,f,g,12] Such interactions relieve electron deficiency at the metal center. Rothwell and co-workers compared NMR data for $Zr(CH_2Ph)_4$ and $Zr(OAr)(CH_2Ph)_3$ (OAr = bulky aryloxide), which contain distorted η^n-benzyl groups, with data for $Zr(OAr)(OAr')(CH_2Ph)_2$, which contains normal σ-bonded benzyl ligands, and noted that η^n-benzyl ligands are characterized by (i) high-field shifts of the ^{13}C CH_2 ($\delta < 75$) and ^1H ortho hydrogen ($\delta < 6.8$) resonances and (ii) large J_{CH} values for the CH_2 group ($J > 130$ Hz). Similar trends have been noted in other η^n-benzyl systems.[12] For example, high-field ^{13}C

(12) (a) Davies, G. R.; Jarvis, J. A. J.; Kilbourn, B. T.; Pioli, A. J. P. *J. Chem. Soc. D* **1971**, 677. (b) Davies, G. R.; Jarvis, J. A. J.; Kilbourn, B. T. *J. Chem. Soc. D* **1971**, 1511. (c) Bassi, I. W.; Allegra, G.; Scordamaglia, R.; Chioccola, G. *J. Am. Chem. Soc.* **1971**, *93*, 3787. (d) Girolami, G. S.; Wilkinson, G.; Thornton-Pett, M.; Hursthouse, M. B. *J. Chem. Soc., Dalton Trans.* **1984**, 2789. (e) Edwards, P. G.; Andersen, R. A.; Zalkin, A. *Organometallics* **1984**, *3*, 293. (f) Latesky, S. L.; McMullen, A. K.; Niccolai, G. P.; Rothwell, I. P.; Huffman, J. C. *Organometallics* **1985**, *4*, 902. (g) Scholz, J.; Schlegel, M.; Thiele, K.-H. *Chem. Ber.* **1987**, *120*, 1369.

shifts for the methylene and ipso carbons (δ 44.1, 126.0), a high-field ^1H shift for the ortho hydrogens (δ 6.75), and a large $J_{CH}(CH_2)$ value of 145 Hz are observed for the cationic η^2-benzyl complex $Cp_2Zr(CH_2Ph)(CH_3CN)^+$.[1d,g] The solid-state structure of $Cp^*Ti(CH_2Ph)_3$ reported by Royo and co-workers contains one agostic CH_2Ph ligand, in which both methylene C–H bonds interact with the Ti(IV) center, and two normal undistorted CH_2Ph ligands.[5f,g] This complex also exhibits a high-field ^1H ortho hydrogen resonance (δ 6.57) but exhibits low-field ^{13}C resonances for the methylene and ipso carbons (δ 94.1, 150.0) and a low $J_{CH}(CH_2)$ value (122 Hz).[13]

The NMR data for **3** establish that one or both of the benzyl ligands have distorted η^n type structures, though the precise nature of the distortion(s) is not clear. The ^1H NMR spectrum (THF-d_8, 25 °C) contains an ortho H resonance at δ 6.61, shifted upfield from the remaining Ph signals. The ^{13}C spectrum (THF-d_8, 25 °C) contains CH_2 and ipso carbon resonances at δ 79.7 and 139.8. These parameters are accommodated by both η^n and agostic structures. However, a large J_{CH} value (132 Hz) is observed for the CH_2 group, which clearly favors an η^n distortion. The ^{13}C spectrum is temperature-dependent: the ipso C resonance shifts downfield to δ 148.4 and the remaining Ph resonances shift slightly upfield when the temperature is lowered to −90 °C, but none of the resonances split. These changes may be due to changes in the extent of η^n-benzyl bonding and THF coordination.

The ^1H NMR spectrum of **3** in THF-d_8 solution at 25 °C contains resonances for 1 equiv of free THF, which establishes that isolated **3** contains 1 equiv of THF and that exchange of free and coordinated THF is rapid on the laboratory time scale. The ^{13}C NMR spectrum of **3** at −90 °C does not show resonances for coordinated THF-d_8. This indicates that exchange of free and coordinated THF-d_8 is rapid on the NMR time scale and precludes determination of the number and nature of coordinated THF ligands in solution.

The observations that (i) isolated **3** contains one THF ligand (rather than two as in **1**, or three) and (ii) the IR spectrum (Nujol) of **3** does not contain low-frequency ν_{CH} bands suggest that the benzyl ligands are also distorted in an η^n manner in the solid state. A structure containing two η^2-benzyl ligands and one THF ligand would be effectively 6-coordinate, analogous to the structure of **2**.

Summary. Cationic mono-Cp* complexes $Cp^*Zr(R)_2(L)_n^+$ are accessible by Cp'_2Fe^+-induced oxidative cleavage of R ligands from neutral $Cp^*Zr(R)_3$ complexes. Both square-pyramidal structures, as observed for $Cp^*Zr(CH_3)_2(THF)_2^+$ (**1**), and octahedral structures, as observed for $Cp^*Zr(dmpe)(CH_3)_2(THF)^+$ (**2**), are possible for this class of complex. These cationic complexes contain highly electrophilic Zr(IV) centers, as evidenced by the rapid decomposition of **1** in CH_2Cl_2 and the decomposition of **3** in THF, the latter probably via Ph^- abstraction from BPh_4^-. Complexes **1** and **3** are formally 14- and 12-electron complexes, respectively, but are stabilized by Zr–O π-bonding and by Zr–Ph interactions. Both of these interactions are probably quite weak, however, given the apparent strong steric influence on the THF ligation in **1** and the fluxionality of both complexes in solution.

Our future work in this area will focus on the chemistry of **1–3** and the synthesis of related complexes that are stable and soluble in less coordinating solvents in which insertion chemistry is favored.

(13) The solid-state structures of most polybenzyl complexes contain several benzyl ligands that are distorted to different degrees; the complexes are usually fluxional in solution, so the NMR parameters are averaged values.

Experimental Section

General Procedures. All manipulations were performed on a high-vacuum line or in a glovebox under a purified N_2 atmosphere. Solvents were distilled from Na/benzophenone. Both Cp^*ZrMe_3 and Cp^*ZrBz_3 were synthesized by the method of Wolczanski and Bercaw.[5a] $[Cp'_2Fe][BPh_4]$ was synthesized by oxidation of Cp'_2Fe by H_2SO_4 and ion exchange with $Na[BPh_4]$.[5g] dmpe ($Me_2PCH_2CH_2PMe_2$) was purchased from Strem and used without further purification. NMR spectra were recorded on a Bruker WM 360-MHz instrument. The ^{13}C NMR assignments were confirmed by DEPT and/or gated-decoupled spectra. Chemical analyses were performed by either Schwarzkopf Laboratory or Analytische Laboratorien. NMR spectra of **1**, **2**, and **3** contain normal BPh_4^- resonances as follows: ^1H NMR (THF-d_8, 360 MHz, 25 °C) δ 7.29 (s, 8 H, ortho), 6.88 (t, J = 7.2 Hz, 8 H, meta), 6.75 (t, J = 7.2 Hz, 4 H, para); ^{13}C NMR (THF-d_8, 91 MHz, 25 °C) δ 164.7 (q, J_{CB} = 49 Hz, ipso), 136.8 125.5, 121.9.

$[Cp^*ZrMe_2(THF)_2][BPh_4]$ (1). THF (100 mL) was vacuum-transferred to a mixture of Cp^*ZrMe_3 (4.90 g, 18.1 mmol) and $[Cp'_2Fe][BPh_4]$ (9.64 g, 18.1 mmol) at −78 °C. The reaction mixture was stirred and warmed to ambient temperature over a period of 1.5 h. Half of the THF was removed under vacuum, and 75 mL of Et_2O was added by vacuum transfer at −78 °C, resulting in precipitation of **1**. The solid product was collected by filtration and washed three times with the THF/Et_2O mixture. The off-white solid was dried under high vacuum for 12 h (yield 9.10 g, 70.3%). Recrystallization from a 90/10 THF/Et_2O solution cooled to −30 °C resulted in amber crystals, which were dried under vacuum for 24 h to yield off-white **1** (55%). Crystals suitable for X-ray diffraction were grown from a saturated THF/Et_2O (ca. 90/10) solution cooled to −35 °C. Elemental analyses of two spectroscopically pure samples gave values for carbon 1–2% lower than the calculated value. The better analysis is reported. Anal. Calcd for $C_{44}H_{57}BO_2Zr$: C, 73.40; H, 7.98; Zr, 12.67. Found: C, 72.33; H, 7.73; Zr, 12.90. ^1H NMR (THF-d_8, 360 MHz, 25 °C): δ 3.62 (m, 8 H, free THF), 1.97 (s, 15 H, C_5Me_5), 1.77 (m, 8 H, free THF), 0.14 (s, 6 H, ZrMe). $^{13}C\{^1H\}$ NMR (THF-d_8, 91 MHz, 25 °C): δ 123.5 (C_5Me_5), 66.2 (free THF), 50.5 (J_{CH} = 117 Hz from gated-decoupled ^{13}C spectrum, ZrMe), 26.4 (free THF), 11.6 (C_5Me_5).

$[Cp^*ZrMe_2(dmpe)(THF)][BPh_4]$ (2). A mixture of **1** (1.00 g, 1.39 mmol) and dmpe (0.760 g, 5.07 mmol) in 20 mL of THF was stirred at ambient temperature for 4 h. Diethyl ether (10 mL) was added by vacuum transfer at −78 °C. The reaction mixture was warmed to ambient temperature with stirring, which resulted in precipitation of **2**. The solid was collected by filtration, washed with 30 mL of hexane, and dried for 12 h under vacuum to yield 0.94 g (82%) of complex **2**, which contained 0.4 equiv of excess THF (^1H NMR) that was not removed after 24 h of drying under high vacuum. Crystals suitable for X-ray diffraction were obtained from saturated THF solutions cooled to −35 °C. Anal. Calcd for $C_{46}H_{65}BOZrP_2 \cdot 0.4THF$: C, 69.15; H, 8.31; P, 7.49. Found: C, 69.67; H, 8.57; P, 7.13. ^1H NMR (THF-d_8, 360 MHz, −56 °C): δ 3.62 (m, 5.6 H, free THF), 2.0–1.85 (m, PCH_2CH_2P, partially obscured by C_5Me_5), 1.95 (s, ca. 15 H, C_5Me_5), 1.78 (m, ca. 5.6 H, free THF), 1.21 (d, 6 H, J_{PH} = 5.5 Hz, PMe), 1.12 (d, 6 H, J_{PH} = 6.6 Hz, PMe), −0.19 (t, J = 9.2 Hz, 6 H, ZrMe). ^1H NMR (THF-d_8, 360 MHz, 39 °C): δ 3.62 (m, 5.6 H, free THF), 2.0–1.8 (m, PCH_2CH_2P, partially obscured by C_5Me_5), 1.95 (s, ca. 15 H, C_Me_5), 1.77 (m, ca. 5.6 H, free THF), 1.13 (br s, 12 H, PMe), −0.17 (t, J = 9.0 Hz, 6 H, ZrMe). $^{13}C\{^1H\}$ NMR (THF-d_8, 91 MHz, −45 °C): δ 121.6 (C_5Me_5), 73.6 (m, coordinated THF-d_8), 66.2 (free THF), 34.0 (J_{CH} = 115 Hz from gated-decoupled ^{13}C spectrum, ZrMe), 29.7 (m, $PCH)_2$, 26.4 (free THF), 25.4 (PCH_2 obscured by THF-d_8 and confirmed by DEPT), 12.0 (C_5Me_5), 11.4 (d, J_{PC} = 12.7 Hz, PMe), 11.1 (d, J_{PC} = 8.9 Hz, PMe). DEPT (THF-d_8, 91 MHz, −53 °C, partial listing): δ 29.7 (dd, PCH_2, outer separation 32 Hz, inner separation 7 Hz), 25.4 (dd, PCH_2, outer separation 24 Hz, inner separation 10 Hz). $^{13}C\{^1H\}$ NMR (THF-d_8, 75.5 MHz, 23 °C): δ 122.4 (C_5Me_5), 68.2 (free THF), 34.6 (br s, ZrMe), 12.0 (C_5Me_5), 11.8 (d, J_{PC} = 10.6 Hz, PMe), PCH_2CH_2P resonances not observed presumably due to exchange broadening. $^{31}P\{^1H\}$ NMR (THF-d_8, 146 MHz, −53 °C): δ −9.7 (d, J_{PP} = 11.4 Hz), −10.0

(d, J_{PP} = 11.4 Hz). $^{31}P\{^1H\}$ NMR (THF-d_8, 146 MHz, 40 °C): δ −9.95 (br s).

A consistent impurity (ca. 1%) is observed in all samples of **2**. This may be an isomer of **2** having cis Zr–Me ligands and axial/equatorial coordination of dmpe. Control experiments establish that this species is not a hydrolysis product of **2**. NMR resonances detected in addition to those of **2** are as follows: ^1H NMR δ 12.22 (C_5Me_5); $^{13}C\{^1H\}$ NMR δ 12.0 (C_5Me_5); $^{31}P\{^1H\}$ NMR δ 2.36 (d, J_{PP} = 31 Hz, PMe), −17.2 (d, J_{PP} = 31 Hz, PMe).

[Cp*Zr(CH_2Ph)$_2$(THF)][BPh_4] (3). THF (150 mL) was vacuum-transferred to a mixture of Cp*Zr(CH_2Ph)$_3$ (2.20 g, 4.40 mmol) and [Cp′$_2$Fe][BPh_4] (2.34 g, 4.40 mmol) at −78 °C. The reaction mixture was warmed to 0 °C and stirred for 1 h, and the solvent was removed under vacuum. The resulting solid was washed with toluene (3 × 25 mL) and dried under vacuum for 24 h (3.10 g, 87.5%). The bright yellow product was purified by recrystallization from THF/hexane or THF/Et_2O. The thermal instability of **3** precluded elemental analysis. ^1H NMR (THF-d_8, 360 MHz, 25 °C): δ 7.33–7.28 (m, partially obscured by m BPh, ca. 4 H), 7.15 (t, J = 7.4 Hz, 2 H, p Ph), 6.61 (d, J = 7.4 Hz, 4 H, o Ph), 3.62 (m, 4 H, free THF), 2.10 (s, 4 H, $ZrCH_2$), 2.07 (s, 15 H, C_5Me_5), 1.78 (m, 4 H, free THF). $^{13}C\{^1H\}$ NMR (THF-d_8, 360 MHz, 25 °C): δ 139.8 (ipso Ph), 131.7 (o Ph), 130.3 (m Ph), 127.6 (p Ph), 125.6 (C_5Me_5), 79.7 (J_{CH} = 132 Hz from gated-decoupled ^{13}C, $ZrCH_2$), 68.2, 26.4 (free THF), 12.1 (C_5Me_5). $^{13}C\{^1H\}$ NMR (THF-d_8, 360 MHz, −91 °C): δ 148.4 (ipso Ph), 129.6 (o Ph), 127.0 (m Ph), 123.4 (p Ph), 122.0 (C_5Me_5), 75.0 ($ZrCH_2$), 68.2, 26.7 (free THF), 12.2 (C_5Me_5).

X-ray Diffraction Studies of 1 and 2. Diffraction data were obtained with an Enraf-Nonius CAD4 diffractometer, and all calculations were made by using the DDP package provided with this system.[14] Crystallographic data are summarized in Table V.

For **1**, after anisotropic refinement on the cation and isotropic refinement on the anion, difference electron density maps showed 50 of the 57 hydrogens, including all 6 of the $ZrCH_3$ hydrogens. In the final refinement stages, the $ZrCH_3$ hydrogen positions were idealized with C–H distances of 0.95 Å and H–C–H angles of 109.5°, the remaining hydrogens were placed at calculated positions, and all hydrogen positions were fixed. When this refinement converged, the $ZrCH_3$ hydrogens were removed, and after two additional refinement cycles a difference electron density map was calculated. All six $ZrCH_3$ hydrogens appeared close to their original positions. The H–C–H angles range from 98 to 110° for C31 and 109 to 118° for C32. The Zr–C31–H angles range from 107 to 121°, and the Zr–C32–H angles range from 102 to 106°. The $ZrCH_3$ hydrogen positions were again idealized and the final refinement steps carried out.

Crystals of **2** contain uncoordinated (free) THF in the lattice. This free THF appears to be disordered between two locations with less than full occupancy. The considerable decline in the intensities of reference reflections may be due in part to loss of free THF from the crystal. The second disordered free THF position appeared after the first free THF was added to the calculation model. As occupancy and temperature factors are strongly correlated, and as the two sets of partially occupied positions are too close for resolution, the refinement was finally carried out with both idealized (free) THF molecules in fixed positions (with orientation and center of gravity fitted to the original orientations found on difference maps). Only the temperature factors of the non-hydrogen atoms of these free THF molecules were varied. Occupancies of 0.25 for each disordered free THF give reasonable temperature factors for the free THF. NMR and analytical results indicate that **2** contains 0.4 equiv of excess THF.

Acknowledgment. This work was supported by DOE Grant DE-FG02-88ER13935 and the Iowa EARDA program. NMR spectra were obtained in the University of Iowa High Field NMR Facility. R.F.J. gratefully acknowledges a Sloan Foundation Research Fellowship and a Union Carbide Research Innovation Award.

Supplementary Material Available: Tables of complete bond angles and lengths, anisotropic thermal parameters, and hydrogen atom coordinates for **1** and **2** (12 pages); listings of structure factors for **1** and **2** (21 pages). Ordering information is given on any current masthead page.

(14) Frenz, B. A. The Enraf-Nonius CAD4 SDP System. In *Computing in Crystallography*; Delft University Press: Delft, Holland, 1978; p 64.